NASA TECHNICAL MEMORANDUM

NASA TM X-71948

COPY NO.

NASA TM X-71948

DEBOND PROPAGATION IN COMPOSITE REINFORCED METALS

by G. L. Roderick*
R. A. Everett*
J. H. Crews, Jr.**

Langley Research Center
Hampton, Virginia

Presented at the ASTM Symposium on Fatigue of Composite Materials, Dec. 2-7, 1973, Bal Harbour, FL

* United States Army Air Mobility
Research and Development Laboratory

** National Aeronautics and Space Administration

NATIONAL AERONAUTICS AND SPACE ADMINISTRATION
LANGLEY RESEARCH CENTER, HAMPTON, VIRGINIA 23665

26

1. Report No.	2. Government Accession No.	3. Recipient's Catalog No.
NASA TM X-71948		

4. Title and Subtitle	5. Report Date
DEBOND PROPAGATION IN COMPOSITE REINFORCED METALS	February 1974
	6. Performing Organization Code

7. Author(s)	8. Performing Organization Report No.
G. L. Roderick; R. A. Everett; and J. H. Crews, Jr.	
	10. Work Unit No. 501-22-02-01-00

9. Performing Organization Name and Address	11. Contract or Grant No.
United States Army Air Mobility Research and Development Laboratory NASA Langley Research Center Hampton, VA 23665	
	13. Type of Report and Period Covered Technical Memorandum

12. Sponsoring Agency Name and Address	14. Sponsoring Agency Code
National Aeronautics and Space Administration Washington, D.C. 20546	

15. Supplementary Notes

Paper presented at ASTM Symposium on Fatigue of Composite Materials, Dec. 2-7, 1973, Bal Harbour, FL

16. Abstract

Strain energy release rates were used to correlate cyclic debonding between metal sheets and composite reinforcement. An expression for the strain energy release rate was derived and applied to fatigue test results for three material systems: graphite bonded to aluminum with both a room temperature and an elevated temperature curing adhesive, and S-glass bonded to aluminum with an elevated temperature curing adhesive. For each material system, several thicknesses were tested with a range of fatigue loads. Cyclic debonding was monitored using a photoelastic technique. A close correlation was found between the observed debond rates and the calculated strain energy release rates for each material system.

17. Key Words (Suggested by Author(s)) (STAR category underlined)	18. Distribution Statement
Fatigue Tests Fatigue (Materials) Adhesive Bonding Composite Materials Reinforced Plates 32 Structural Mechanics	Unclassified - Unlimited

19. Security Classif. (of this report)	20. Security Classif. (of this page)	21. No. of Pages	22. Price*
Unclassified	Unclassified	16	$3.00

*Available from { The National Technical Information Service, Springfield, Virginia 22151
STIF/NASA Scientific and Technical Information Facility, P.O. Box 33, College Park, MD 20740

ABSTRACT

Strain energy release rates were used to correlate cyclic debonding between metal sheets and composite reinforcement. An expression for the strain energy release rate was derived and applied to fatigue test results for three material systems: graphite bonded to aluminum with both a room temperature and an elevated temperature curing adhesive, and S-glass bonded to aluminum with an elevated temperature curing adhesive. For each material system, specimens of several thicknesses were tested with a range of fatigue loads. Cyclic debonding was monitored using a photoelastic technique. A close correlation was found between the observed debond rates and the calculated strain energy release rates for each material system.

INTRODUCTION

Adhesive bonding is becoming widely used in aircraft structures for joining structural components and for making efficient materials. In joints, it eliminates severe stress concentrations that are usually introduced with mechanical fasteners. Although it can be advantageous in metal-to-metal joints, it is particularly applicable to joining composite materials, whose static strength is very sensitive to stress concentrations. Also, bonding is used to make more efficient structures by joining separate materials to form one system. For example, hybrid systems, formed by bonding metal and composite layers, have higher static strength--for equal weight and stiffnesses [1]--than metals while being more reliable than composites alone. Indeed, composites themselves derive their high efficiency from bonded collections of constituent materials.

When these bonded structures are subject to fatigue loading they may be susceptible to a little-considered mode of fatigue failure; cyclic debonding [2]. Because most practical structures will be subject to fatigue loading, cyclic debonding should be considered in their design. Unfortunately, a designer has virtually no rationale to account for cyclic debonding; consequently, either the reliability or efficiency of his structure may suffer. As a first step in supplying a design rationale, the objective of this paper is to present a cyclic debond analysis.

The analysis was developed for simple laminated specimens made of aluminum alloy sheet bonded to graphite or fiberglass composites and tested

under constant-amplitude fatigue loading. It is based on the correlation of the observed rate of debonding with the computed rate of strain energy release as the debond extended.

SYMBOLS

The units for the physical quantities defined in this paper are given in the International System of Units (SI) [3]. The measurements and calculations were made in the U.S. Customary Units.

a	Debond length, m
da/dN	Debond propagation rate, m/cycle
c,n	Curve fit parameters
E	Young's modulus, MN/m^2
G	Strain energy release rate, J/m
L	Length, m
P	Applied load, N
R	Ratio of minimum-to-maximum applied stress
S	Stress in composite core of Region A, MN/m^2
t	Thickness, m
ΔT	Change in temperature, K
U	Strain energy, J
V	Volume, m^3
w	Specimen width, m
x,y	Cartesian coordinates, m
α	Thermal expansion coefficient, K^{-1}

δ Deflection, m

ε Strain

σ Stress, MN/m^2

ϕ Strain energy density, J/m^3

Subscripts:

1 Denotes aluminum cover

2 Denotes composite core

A Denotes Region A

B Denotes Region B

C Denotes Region C

EXPERIMENTAL PROCEDURE

Specimens and Loading

The specimen configuration used in the present study is shown in Figure 1. The specimen was composed of two 7075-T6 aluminum alloy sheets bonded to a unidirectional composite core of graphite or S-glass (see Table I). Two bonding materials were used for the graphite core specimens: EPON 927 which cures at room temperature (material system 1), and AF 126 which cures at 394 K (material system 2). The AF 126 was also used to bond the S-glass core specimens (material system 3, see Table II). The abrupt change in section of the specimen purposely introduced a severe stress concentration in the bonding materials. Under cyclic loading, debonding started readily at this high stress concentration.

The specimens were tested axially under constant-amplitude fatigue loading with $R = 0.1$. Maximum stresses in the unreinforced composite core range from 211 to 1210 MN/m^2. All of the tests were performed at a frequenc of 10 Hz.

Measurement of Debond Rates

The debond front was monitored continuously by a photoelastic technique Photoelastic coatings were bonded to the aluminum sheets, and the specimen was viewed through a polarizer and quarter-wave plate. Under loading, isochromatic fringes developed at the debond front due to the high strain gradient in that vicinity. Figure 2 shows the location of the photoelastic coatings on the specimen and typical isochromatic fringes. The isochromatic fringes were photographed at specified load cycle intervals to relate the debond front location to the number of applied load cycles.

STRAIN ENERGY RELEASE RATE EQUATIONS

Fatigue crack propagation rates in metals have been correlated using the strain energy release rate, G, [4] where

$$G = P\left(\frac{d\delta}{da}\right) - \frac{dU}{da} \qquad (1)$$

The term $P(d\delta/da)$ is the work done by the applied load as the crack extends, and dU/da is the change in strain energy as the crack extends. Intuition suggests that a similar correlation may be valid for debond propagation. Consequently, an expression for G was developed for the specimen

configuration used in this study. This expression was determined using a one-dimensional elasticity analysis described by the following discussion.

To simplify the analysis, the specimen was separated into three regions: A, B, and C (figure 3). In Regions A and C only uniform stresses in the x direction are significant. Consequently, these regions could be analyzed by an elementary elasticity method. Region B had a complex stress distribution and could not be analyzed using elementary methods. The stress distribution in Region B was assumed to remain constant as the debond extended. As will be shown, this constancy eliminated the need to calculate the stress distribution in Region B.

An expression for $(d\delta/da)$ in equation (1) was derived from the change in the end deflection of the specimen, $d\delta$, caused by an increment of debonding, da. Before debonding occurred, the end deflection was given by:

$$\delta = \delta_A + \delta_B + \delta_C \tag{2}$$

and after debonding by:

$$\delta' = \delta_A' + \delta_B + \delta_C' \tag{3}$$

The stress distribution in Region B was assumed to be the same before and after the region translated; thus, the δ_B term did not change with debonding. To find $d\delta$, equation (2) was subtracted from equation (3) yielding:

$$\delta' - \delta = d\delta = (\delta_A' - \delta_A) + (\delta_C' - \delta_C) \tag{4}$$

The deflections on the right side of equation (4) can be expressed in the general form:

$$\delta = \varepsilon L \tag{5}$$

Substitution of equation (5) into equation (4) yields:

$$d\delta = [\varepsilon_A(L_A + da) - \varepsilon_A L_A] + [\varepsilon_C(L_C - da) - \varepsilon_C L_C] \tag{6}$$

$$d\delta = (\varepsilon_A - \varepsilon_C)da \tag{7}$$

or

$$\frac{d\delta}{da} = (\varepsilon_A - \varepsilon_C) \tag{8}$$

The expression for dU/da in equation (1) was derived by calculating the change of strain energy in the specimen, dU, resulting from an increment of debonding da. Employing the same reasoning used in the development of equation (4), the change in strain energy is:

$$U' - U = dU = (U_A' - U_A) + (U_C' - U_C) \tag{9}$$

The strain energies on the right side of equation (9) can be expressed in the general form:

$$U = \phi V \tag{10}$$

Substitution of equation (10) into equation (9) yields:

$$dU = \{\phi_{A2} wt_2 (L_A + da) - \phi_{A2} wt_2 L_A\}$$

$$+ \{[2\phi_{C1} wt_1 (L_C - da) + \phi_{C2} wt_2 (L_C - da)]$$

$$- [2\phi_{C1} wt_1 L_C + \phi_{C2} wt_2 L_C]\} \qquad (11)$$

$$dU = w[\phi_{A2} t_2 - (\phi_{C2} t_2 + 2\phi_{C1} t_1)]da \qquad (12)$$

or

$$\frac{dU}{da} = w[\phi_{A2} t_2 - (\phi_{C2} t_2 + 2\phi_{C1} t_1)] \qquad (13)$$

Substitutions of equations (8) and (13) into equations (1) yields:

$$G = P(\varepsilon_A - \varepsilon_C) - w[\phi_{A2} t_2 - (\phi_{C2} t_2 + 2\phi_{C1} t_1)] \qquad (14)$$

This equation is evaluated in the appendix in terms of applied stress, temperature change, material parameters, and specimen configuration and leads to

$$G = \frac{t_1 t_2 E_1 w}{E_2(2t_1 E_1 + t_2 E_2)} [S - \Delta T(\alpha_1 - \alpha_2)E_2]^2 \qquad (15)$$

RESULTS AND DISCUSSIONS

Figure 4 shows a sample plot of debond length against the number of applied load cycles. The shape of this debond curve was typical for all three material systems tested. Initially, debonding was nonlinear with respect to the number of applied load cycles, but became linear as the debond progressed. The main focus of this paper is on the linear portion of the debond behavior; however, a brief discussion of the nonlinear region is merited.

Nonlinear debonding occurred when the debond front was near the change in cross section of the specimen. The texture of the failure surface indicates that the failure mechanism changed as the debond extended. Figure 5 shows a photograph of the fracture surface of a typical debond specimen of material system 2. The graphite-composite core is shown on the left and the mating aluminum cover sheet on the right. As the photograph indicates, the failure mechanism was initially cohesive, but changed to predominantly adhesive as the debond extended. Similar behavior was observed for material system 3. However, for material system 1 the failure mechanisms seemed to be reversed; initially the failure was adhesive, but changed to cohesive as the debond extended. For all three material systems the nonlinear portion of the debond behavior seemed to be related to a transition in failure mechanism.

Debond propagation rates were determined from the linear portion of debond versus cycle plot for each specimen. Figure 6 is a plot of rate against G, equation (15), for the three material systems. This figure

shows debond rate to be a single valued function of G for all material thicknesses. Table 3 presents these data in tabular form. An equation of a form which had successfully correlated fatigue crack propagation data for isotropic metals [5] is:

$$\frac{da}{dN} = c(G)^n \tag{16}$$

This equation fits the data in figure 6 quite well (dashed curves). The constants c and n were determined using least-squares techniques and are given in the following table:

Material System	c	n
1	1.19×10^{-9}	3.30
2	2.32×10^{-9}	2.15
3	5.63×10^{-9}	3.76

Equation (16) may be useful to predict debond rates in composite reinforced structures subjected to fatigue loading for the systems studied. However, for other materials systems, appropriate values of c and n must be obtained from cyclic test data.

Figure 6 shows that c and n differ for each material system. This difference was probably due to the different bond strength and residual thermal stress of each system. The residual thermal stress in the graphite aluminum specimens bonded at elevated temperature was calculated to be as high as 120 MN/m^2 in the graphite core. Because residual thermal stresses of this magnitude are significant in comparison to the applied stress in

the core, they were included in the derivation of the strain energy release rate. However, because both the residual thermal stresses and bond strength differed from system to system, isolation of either effect was not possible for the limited tests reported here.

CONCLUDING REMARKS

A fatigue analysis method was developed for cyclic debonding of laminates composed of metal and composite layers. The strain energy release rate, G, correlated the debond propagation rates from each of three series of laboratory tests for several applied loads and thicknesses. Specimens tested were graphite bonded to aluminum at room temperature, graphite bonded to aluminum at elevated temperature, and S-glass bonded to aluminum at elevated temperature. The test data were well represented by an equation of the form $da/dN = c(G)^n$. For the systems studied, a closed-form expression was developed for G, which included residual thermal stresses.

This study indicates that G promises to be a tractable tool with which to analyze the relations between cyclic debonding and fatigue loading in laminated structures. For simplicity in establishing G as a correlating parameter, tests were restricted to constant amplitude loading at room temperature with a simple geometric configuration. The correlation achieved herein was on specific material systems that may be applicable to aircraft structures. However, to be useful for structural applications the model should be refined and verified for more complex fatigue environments and

for complicated configurations. Also, since high residual thermal stresses may occur for some material systems, their effect on cyclic debonding should be established.

REFERENCES

[1] Johnson, R. W.; and June R. R.: Application Study of Filamentary Composites in a Commercial Jet Aircraft Fuselage. NASA CR-112110, 1972.

[2] Blickfeldt, B.; and McCarty, J. E.: Analytical and Experimental Investigation of Aircraft Metal Structures Reinforced with Filamentary Composites. NASA CR-2039, 1972.

[3] Mechtly, E. A.: The International System of Units. NASA SP-7012, 1969.

[4] Paris, Paul C.; and Sih, George C.: Stress Analysis of Cracks, Fracture Toughness Testing and Other Applications. Spec. Tech. Pub. No. 381, Amer. Soc. Testing Mater., 1965, pp. 30-83.

[5] Paris, Paul C.: The Fracture Mechanics Approach to Fatigue; Sagamore Army Materials Research Conference, Aug. 1963, pp. 116.

[6] Boley, Bruno A.; and Werner, Jeromeh: Theory of Thermal Stresses, Wiley, New York, 1960, pp. 259.

APPENDIX

Development of the Strain Energy Release Rate Equation

The strain energy release rate for debonding of a metal overlayed with a composite (figure 3) was given in the body of this paper by equation (14):

$$G = P(\varepsilon_A - \varepsilon_C) - w[\phi_{A2}t_2 - (\phi_{C2}t_2 + 2\phi_{C1}t_1)] \tag{A1}$$

The strains in equation (A1) were found by requiring equilibrium, strain compatability, and a constitutive relation between stress and strain in regions A and C. Equilibrium is satisfied by:

$$P = w\int\sigma dy \tag{A2}$$

For the one dimensional analysis used in this problem, strain compatability was assured by assuming that the strain through the specimen thickness is constant. The constitutive relation for the problem is given as [6]

$$\sigma = E(\varepsilon - \alpha\Delta T) \tag{A3}$$

Using these three relationships, the strains in region A and C can be calculated.

In region A, compatability is satisfied. Equilibrium is satisfied when:

$$P = St_2w = \sigma_{A2}t_2w \tag{A4}$$

The constitutive equation (A3) for this region is:

$$\sigma_{A2} = E_2(\varepsilon_A - \alpha_2 \Delta T) \tag{A5}$$

Substituting equation (A5) into equation (A4) and solving for ε_A yields:

$$\varepsilon_A = \frac{S}{E_2} + \alpha_2 \Delta T \tag{A6}$$

For region C, compatability is satisfied when:

$$\varepsilon_{C1} = \varepsilon_{C2} = \varepsilon_C \tag{A7}$$

Equilibrium is satisfied when:

$$P = St_2 w = 2t_1 w \sigma_{C1} + \sigma_{C2} t_2 w \tag{A8}$$

The constitutive relationships for the metal and composite respectively are:

$$\sigma_{C1} = E_1(\varepsilon_C - \alpha_1 \Delta T) \tag{A9}$$

$$\sigma_{C2} = E_2(\varepsilon_C - \alpha_2 \Delta T) \tag{A10}$$

Substituting equation (A9) and (A10) into equation (A8) and solving for ε_C lead to:

$$\varepsilon_C = \frac{St_2 + \Delta T(2E_1 t_1 \alpha_1 + E_2 t_2 \alpha_2)}{2E_1 t_1 + E_2 t_2} \tag{A11}$$

The strain energy density can be expressed as:

$$\phi = \frac{\sigma^2}{2E} = \frac{[E(\varepsilon - \alpha\Delta T)]^2}{2E}$$

or (A12)

$$\phi = \frac{E}{2}[\varepsilon^2 - 2\varepsilon\alpha\Delta T + \alpha^2(\Delta T)^2]$$

For region A, substituting equation (A6) into equation (A12) yields:

$$\phi_{A2} = \frac{E_2}{2}[\varepsilon_A^2 - 2\varepsilon_A\alpha_2\Delta T + \alpha_2^2(\Delta T)^2] \quad (A13)$$

Similarly for region C, substitution of equation (A11) into equation (A12) for the metal yields:

$$\phi_{C1} = \frac{E_1}{2}[\varepsilon_C^2 - 2\varepsilon_C\alpha_1\Delta T + \alpha_1^2(\Delta T)^2] \quad (A14)$$

and for the composite yields:

$$\phi_{C2} = \frac{E_2}{2}[\varepsilon_C^2 - 2\varepsilon_C\alpha_2\Delta T + \alpha_2^2(\Delta T)^2] \quad (A15)$$

Substitution of equations (A6), (A8), (A11), (A13), (A14), and (A15) into equation (A1) yields:

$$G = \frac{t_1 t_2 E_1 w}{E_2(2t_1E_1 + t_2E_2)}[S - \Delta T(\alpha_1 - \alpha_2)E_2]^2 \quad (A16)$$

the expression for strain energy release rate.

TABLE I. – MATERIAL PROPERTIES

MATERIAL	E	α
	MN/m^2	K^{-1}
7075-T6 ALUMINUM ALLOY	71×10^3	22.5×10^{-6}
GRAPHITE-EPOXY	131×10^3	-0.38×10^{-6}
S-GLASS-EPOXY	61×10^3	3.60×10^{-6}

TABLE 2. – SPECIMEN MATERIAL SYSTEMS

MATERIAL SYSTEM	COMPOSITE	BONDING MATERIAL	BONDING MATERIAL THICKNESS	CURE TEMPERATURE
			mm	K
1	GRAPHITE-EPOXY	EPON 927	0.13	RT(1)
2	GRAPHITE-EPOXY	AF 126	0.13	394
3	S-GLASS-EPOXY	AF 126	0.13	394

(1) RT = 294 K

TABLE 3. – STRAIN ENERGY RELEASE RATES AND CYCLIC DEBOND RATES

MATERIAL SYSTEM TYPE	THICKNESS, mm									
	t_1	t_2								
TYPE 1	.51	0.81	S (1)	504	706	807	1210			
			da/dN (2)	0.000714	0.092	0.146	2.500			
			G (3)	16.1	31.5	41.2	92.6			
	1.02	1.64	S	426	475	527	590	639	698	746
			da/dN	0.0168	0.0229	0.166	0.373	0.498	1.32	1.78
			G	23.6	29.3	36.2	45.3	53.2	63.4	72.4
	1.60	2.50	S	211	270	324	376	429	543	598
			da/dN	0.00689	0.0315	0.0569	0.0785	0.163	1.32	5.59
			G	8.9	14.7	20.8	28.0	36.6	58.6	70.9

(1) STRESS, MN/m^2
(2) DEBOND RATE, μm/cycle
(3) STRAIN ENERGY RELEASE RATE WITH THERMAL RESIDUAL STRESSES, G, joules/meter

TABLE 3. – CONCLUDED

MATERIAL SYSTEM TYPE	THICKNESS, mm t_1	THICKNESS, mm t_2									
TYPE 2	1.02	1.57	S (1)	390	445	541	605	605	667	667	703	716
			da/dN (2)	0.015	0.0193	0.0302	0.0635	0.0779	0.0815	0.0592	0.0899	0.112
			G (3)	60	70	89	103	103	117	117	126	130
	1.60	2.54	S	325	420	478	490	535	589	631		
			da/dN	0.0279	0.0437	0.065	0.0627	0.0734	0.116	0.144		
			G	78	104	121	125	139	158	173		
TYPE 3	1.02	.86	S	334	390	446	507	558	614	670	725	781
			da/dN	0.0305	0.0607	0.0772	0.184	0.409	0.605	1.26	2.03	2.95
			G	53	67	83	102	119	139	162	185	211
	1.60	1.40	S	217	274	328	384	438	492	547	595	658
			da/dN	0.0078	0.0254	0.0838	0.181	0.546	1.14	1.85	3.33	5.92
			G	47	64	84	105	129	155	184	212	251

(1) STRESS, MN/m^2

(2) DEBOND RATE, μm/cycle

(3) STRAIN ENERGY RELEASE RATE WITH THERMAL RESIDUAL STRESSES, G, joules/meter

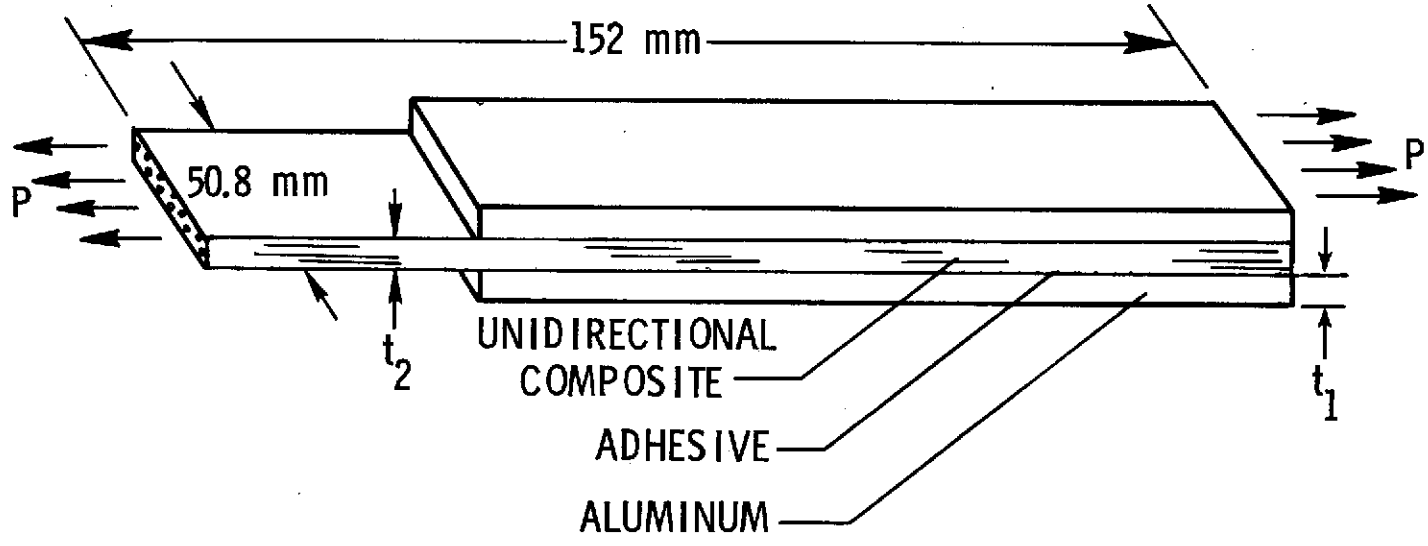

FIGURE 1 - SPECIMEN CONFIGURATION

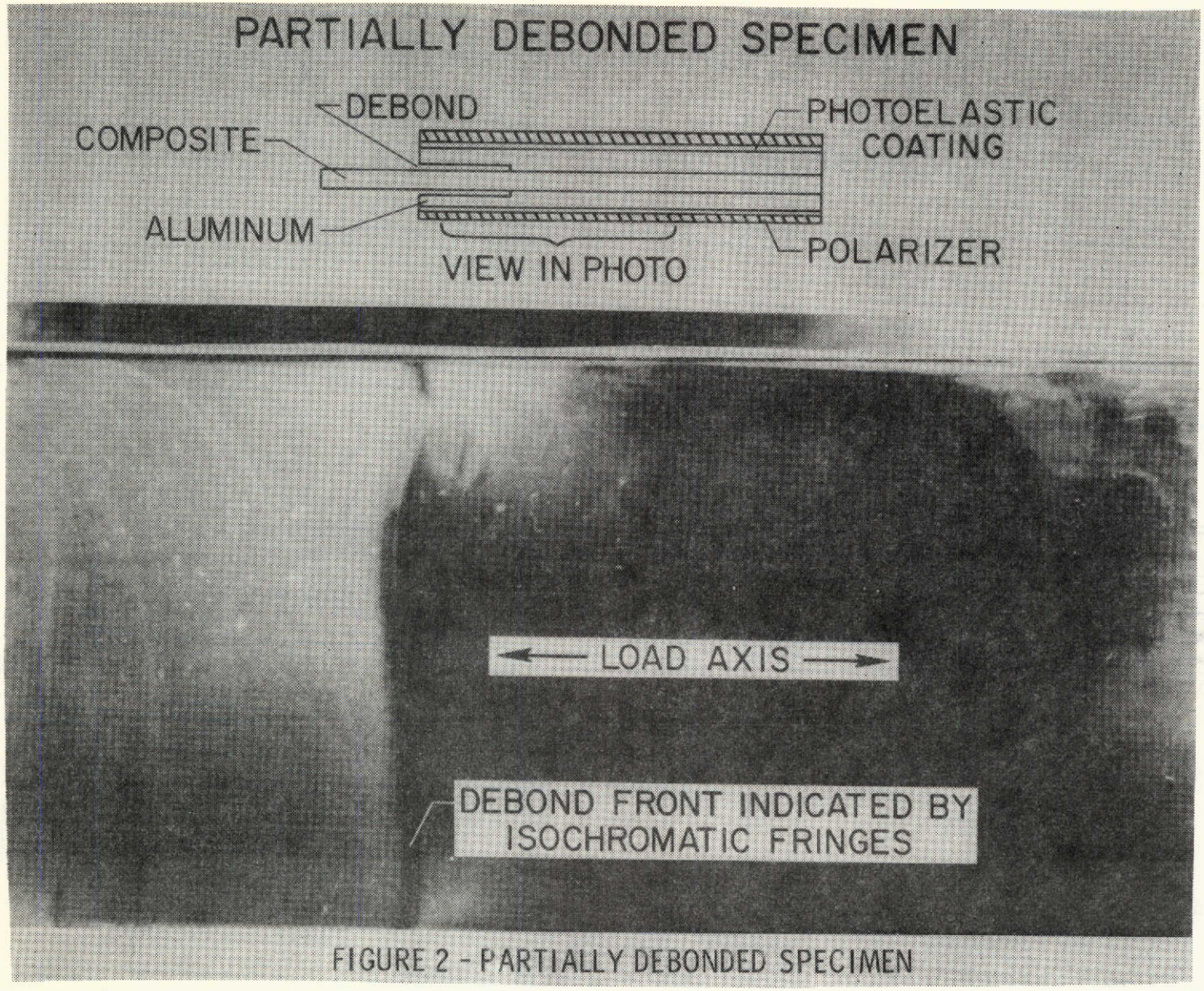

FIGURE 2 - PARTIALLY DEBONDED SPECIMEN

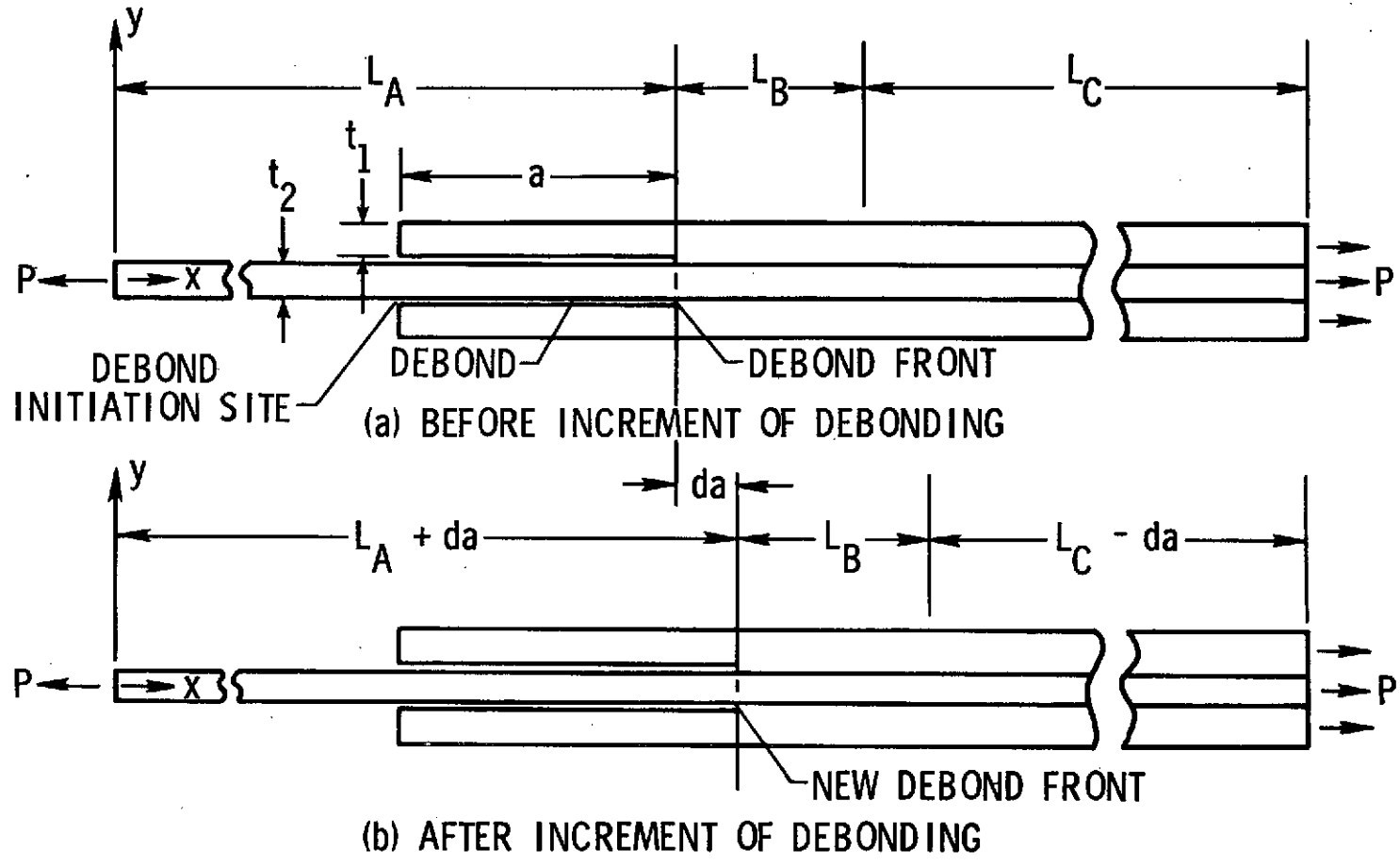

FIGURE 3 - TEST SPECIMEN BEFORE AND AFTER AN INCREMENT OF DEBONDING

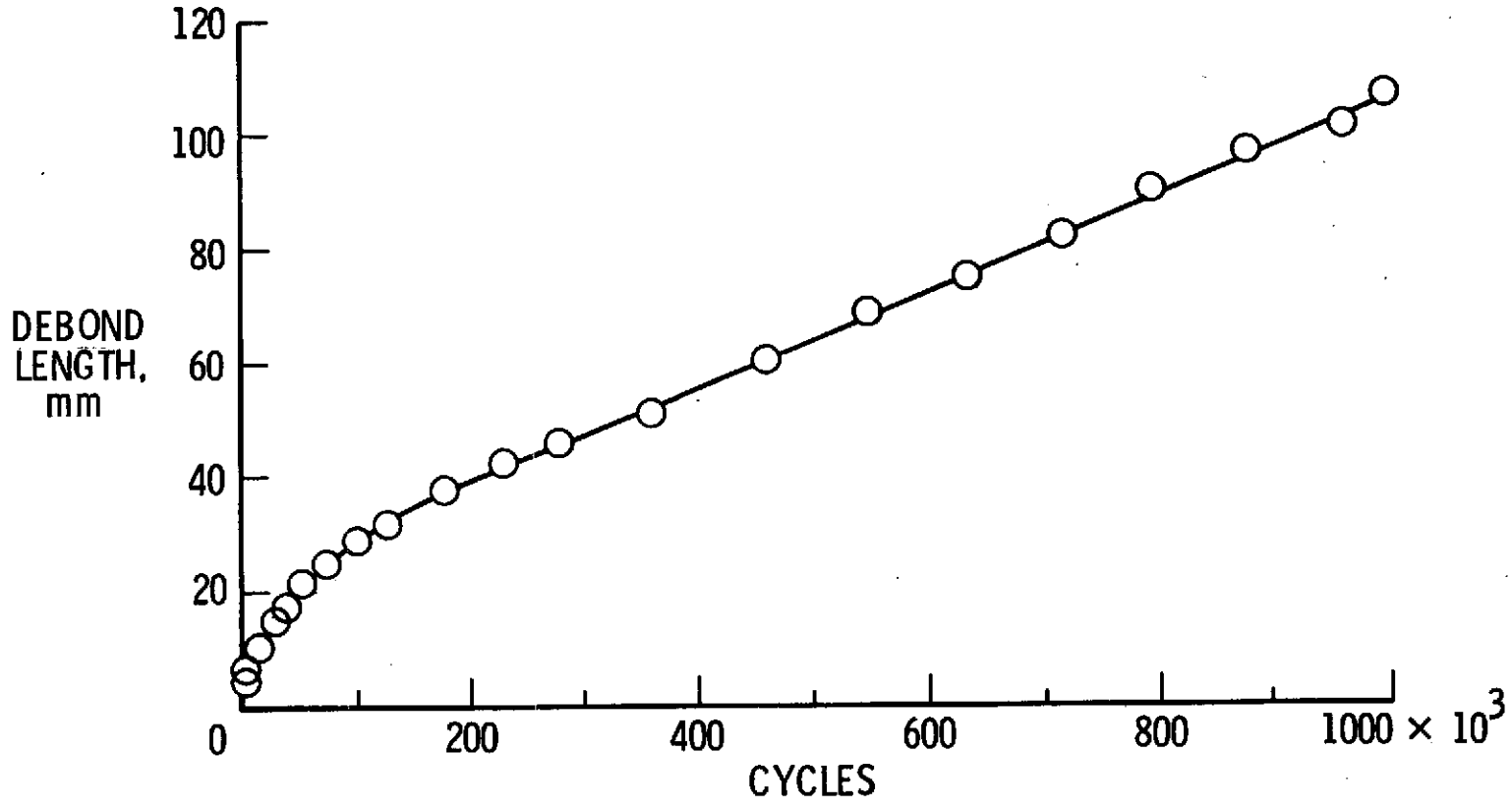

FIGURE 4 - TYPICAL VARIATION OF DEBOND LENGTH WITH CYCLES

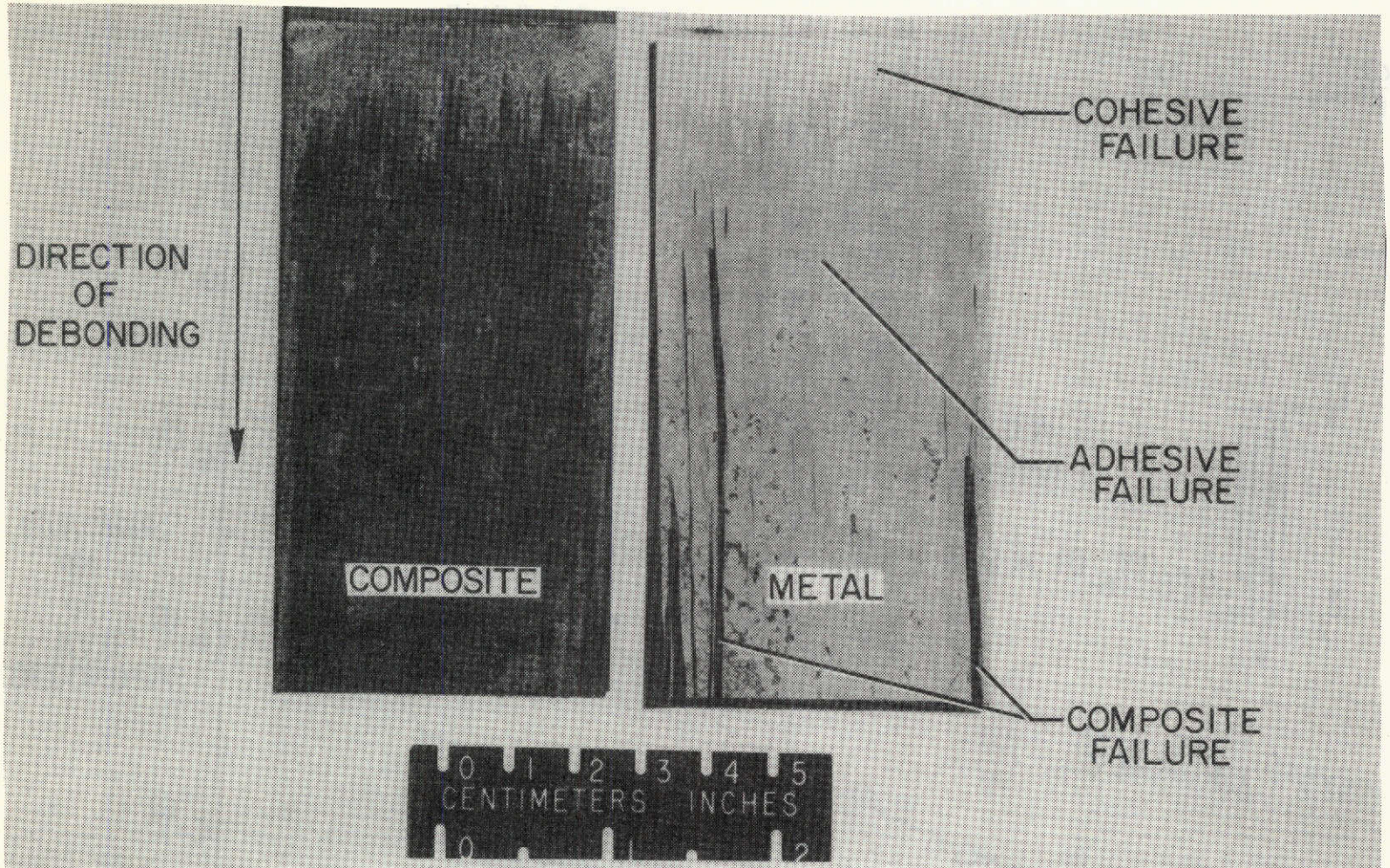

FIGURE 5 - DEBONDED SURFACES OF A MATERIAL TYPE 2 SPECIMEN

A-11

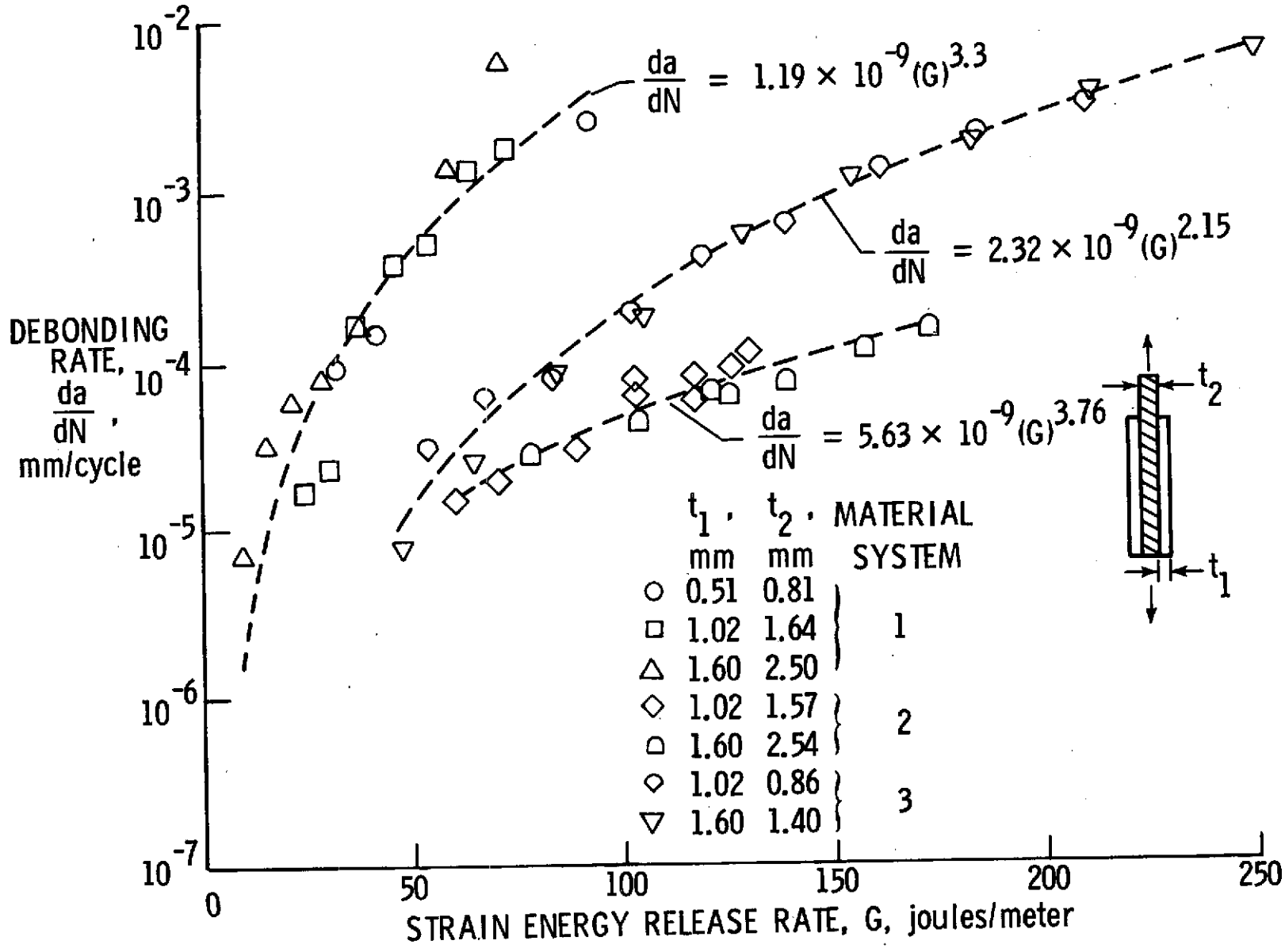

FIGURE 6 - VARIATION OF DEBOND RATE WITH STRAIN ENERGY RELEASE RATE